

Astrophysical light scattering problems (PAP316)

Lectures 5a & 5b

Karri Muinonen

Academy Professor

Department of Physics, University of Helsinki, Finland

Contents

- Introduction
- Methods of modern observations
- Main trends in linear polarization
- In situ measurements
- Distribution of polarization over the coma
- Specific phenomena in linear polarization
- Interpretation of linear polarization data
- Comet nuclei
- Circular polarization
- Similarity and diversity of comets: Classification issues
- Conclusions
- Perspectives

Introduction (1/2)

- Physical characterization of **astronomical objects** (e.g., surfaces of airless planetary objects)
- **Direct problem** of light scattering by particles with varying **particle size, shape, refractive index, and spatial distribution**
- **Inverse problem** based on **astronomical observations and/or experimental measurements**
- Plane of scattering, scattering angle, solar phase angle, degree of linear polarization

Introduction (2/2)

- **Comets**

- low-density km-sized objects of ices (mostly H₂O, CO₂, CO) and dust (silicates, carbon, organics)
- nucleus, coma, tails
- “dirty iceballs” or “icy dustballs”

- **Polarimetry**

- single scattering in cometary comae
- powerful, relevant computational techniques available (Discrete-Dipole Approximation, Superposition T-Matrix Method)
- Experimental measurements using particle flows and microgravity environments

- **Polarimetry**

- major role in cometary science
- nearly full phase-angle coverage
- negative and positive polarization
- classification
- spectral dependence in visible and near-IR
- polarization for forward scattering using Sun-grazers
- nonzero circular polarization with predominantly left-handed helicity
- possibility of combining remote spectrophotometric and polarimetric data with in situ data

Methods of modern observations

- **Aperture polarimetry**
 - dominant before the CCD era
 - broadband filters bring up dust component
 - narrow-band cometary filters allow for separating dust and gas signals
- **Imaging polarimetry**
 - detailed distribution in the comae
 - works well for comets at small geocentric distances
 - broadband filters needed for distant comets
- **Spectro-polarimetry**
 - long-slit polarimetry rare for comets
 - allows to identify continuum and emission bands
- **Near-IR polarimetry**
 - gas contamination negligible in J, H, K filters
 - many comets observed
- **Spaceborne and in situ polarimetry**
 - SOHO LASCO coronagraph in H-alpha for 96P/Machholz 1
 - Giotto for 1P/Halley and 26P/Grigg-Skjellerup

Main trends in linear polarization

- Phase-angle-dependence of linear polarization in the visible
 - high-polarization vs. low-polarization comets
 - high-polarization comets show similar dependences
 - coma dust particles likely to be similar
 - exceptions: see Fig. 22.1
 - slight dependence on aperture

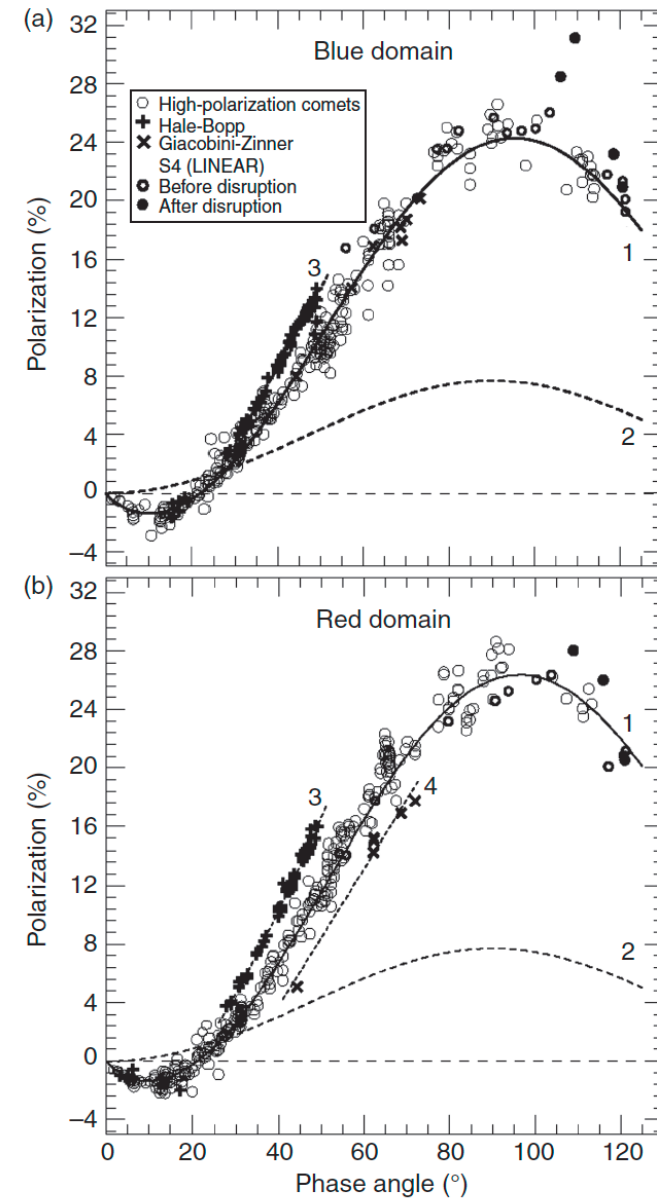


FIGURE 22.1 The phase-angle dependence of polarization for comets in the blue (a) and red (b) continuum. Curve 1 is the fit to data for high- P_{max} comets; curve 2 shows theoretical results for diatomic molecules according to Eq. (1); curve 3 is the fit to the comet Hale-Bopp data; curve 4 is the fit to the comet Giacobini-Zinner data.

- Phase-angle dependences continued
 - large variations in polarization for low-polarization comets, in particular, for $>40^\circ$
 - low-polarization comets show large dependence on aperture: polarization increases with decreasing field of view

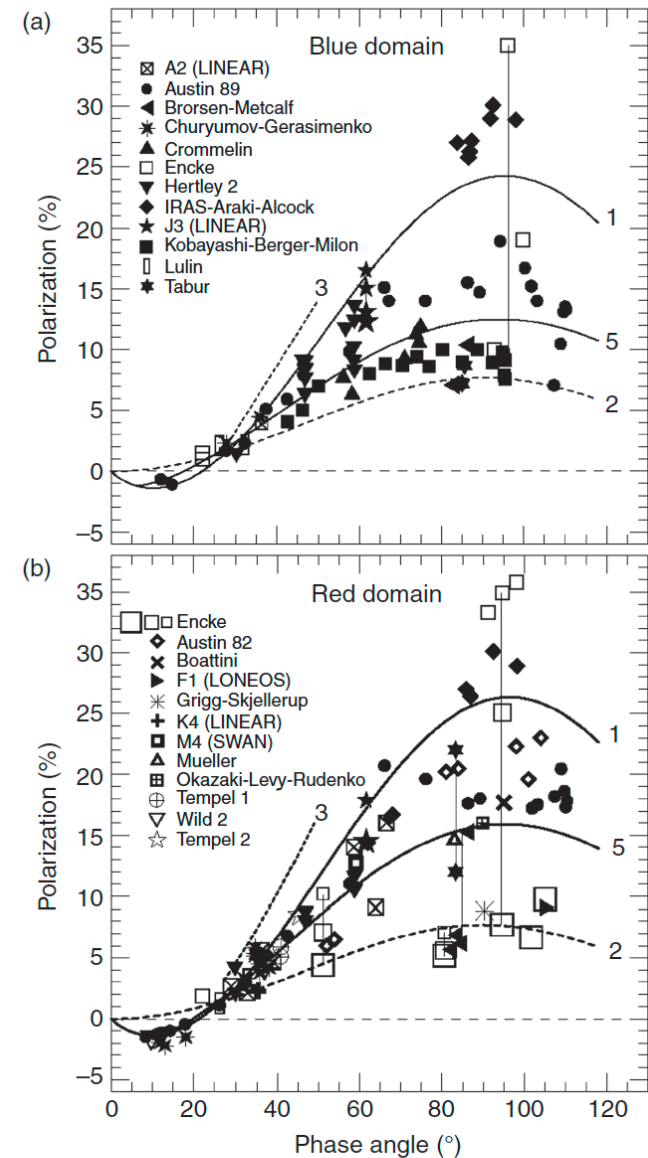


FIGURE 22.2 The polarization vs. phase angle for the low- P_{max} comets in the blue (a) and red (b) continuum. The curves 1, 2, and 3 are the same as in Fig. 22.1. Curves 5 are the fits to all polarization data for low- P_{max} comets with large apertures in the blue and the red. The vertical lines show the dependence of the polarization on aperture size for comets 2P/Encke, D/1996 Q1 (Tabur), and C/1999 J3 (LINEAR) as well as on the bandpass of the red filter for comet 23P/Brorsen-Metcalf.

- Phase-angle dependence in the near-IR
 - for Hale-Bopp, negative polarization branch virtually absent: Rayleigh domain

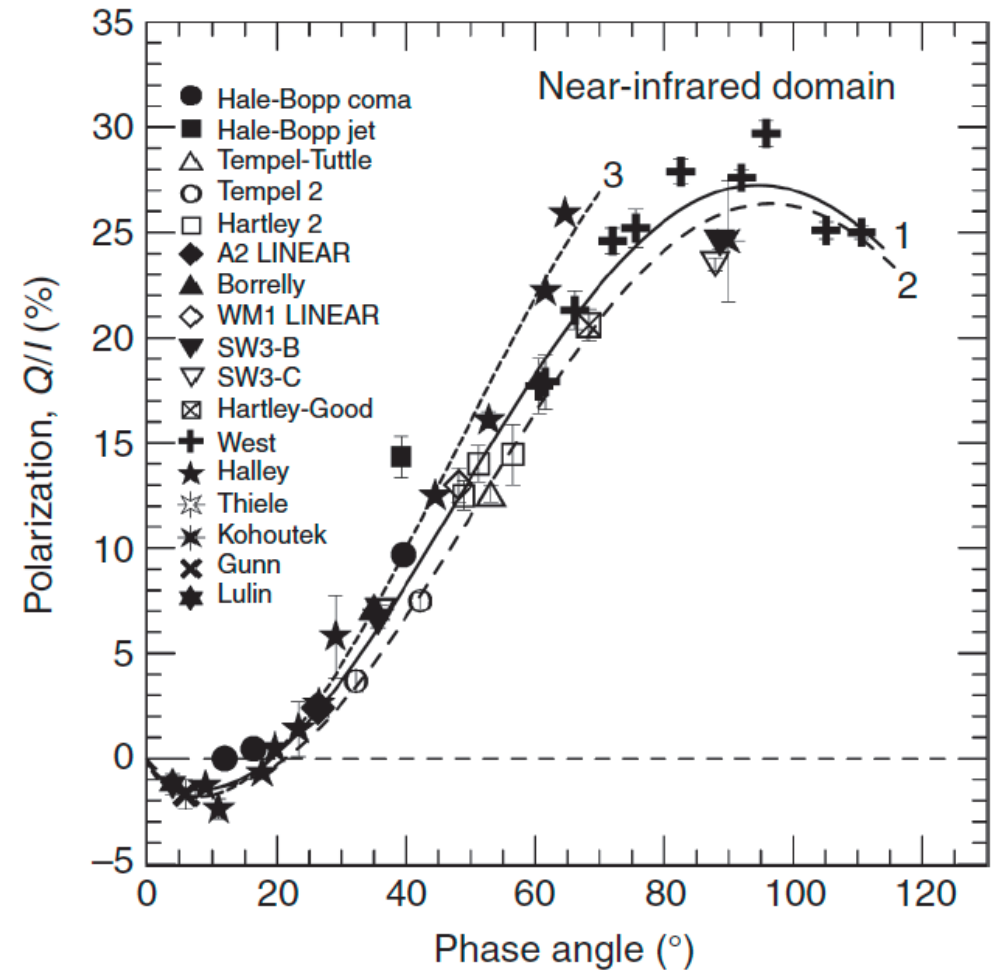


FIGURE 22.3 Phase-angle dependence of polarization for comets in the near-IR. Curve 1 is the average polarization curve for comets in the near-IR; curve 2 is the mean phase dependence of polarization taken from Fig. 22.1(b) for the high- P_{max} comets in the red; curve 3 is the fit to the polarization data of comet Halley in the K band.

- Spectral dependences of polarization
 - in the visible, most comets exhibit increase of polarization with wavelength at 30-80°
 - positive, red polarimetric color
 - the negative branch becomes shallower in the near-IR (again, red polarimetric color)

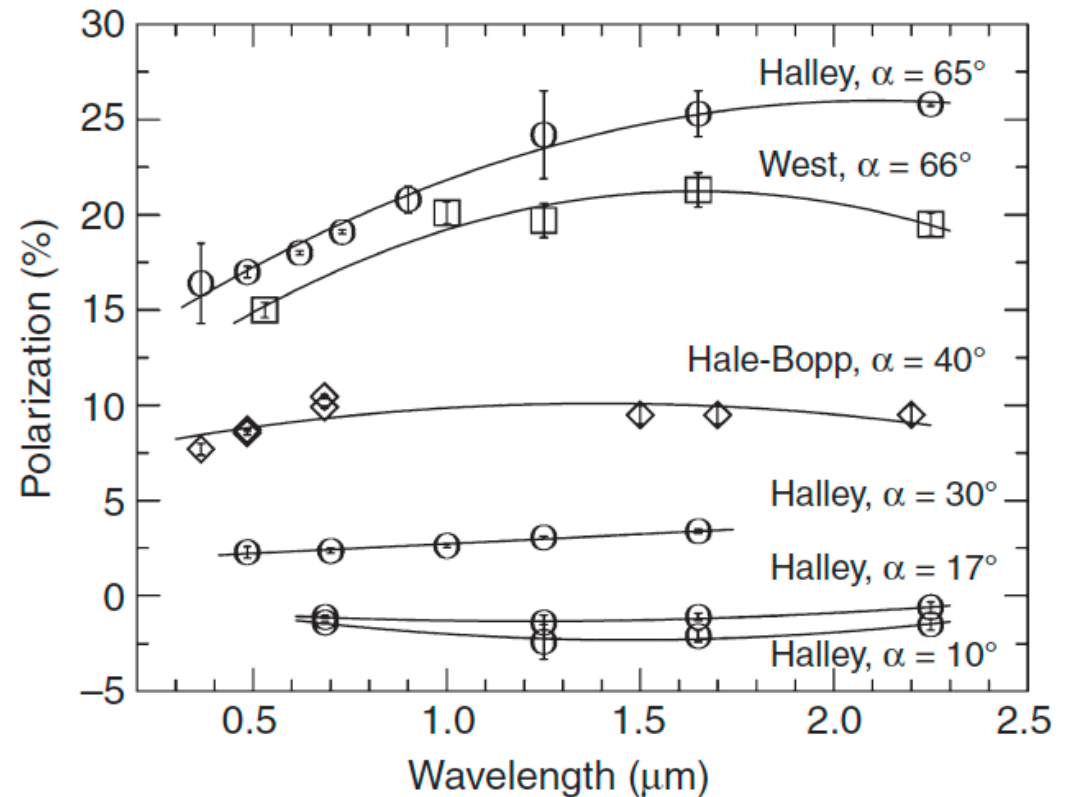


FIGURE 22.4 Typical spectral dependences of polarization for comets C/1975 VI (West), C/1995 OI (Hale-Bopp), and IP/Halley at different phase angles. The curves are polynomial fits.

- Spectral dependences of polarization, exceptions
 - decreasing polarization with wavelength for 38-60° for five comets

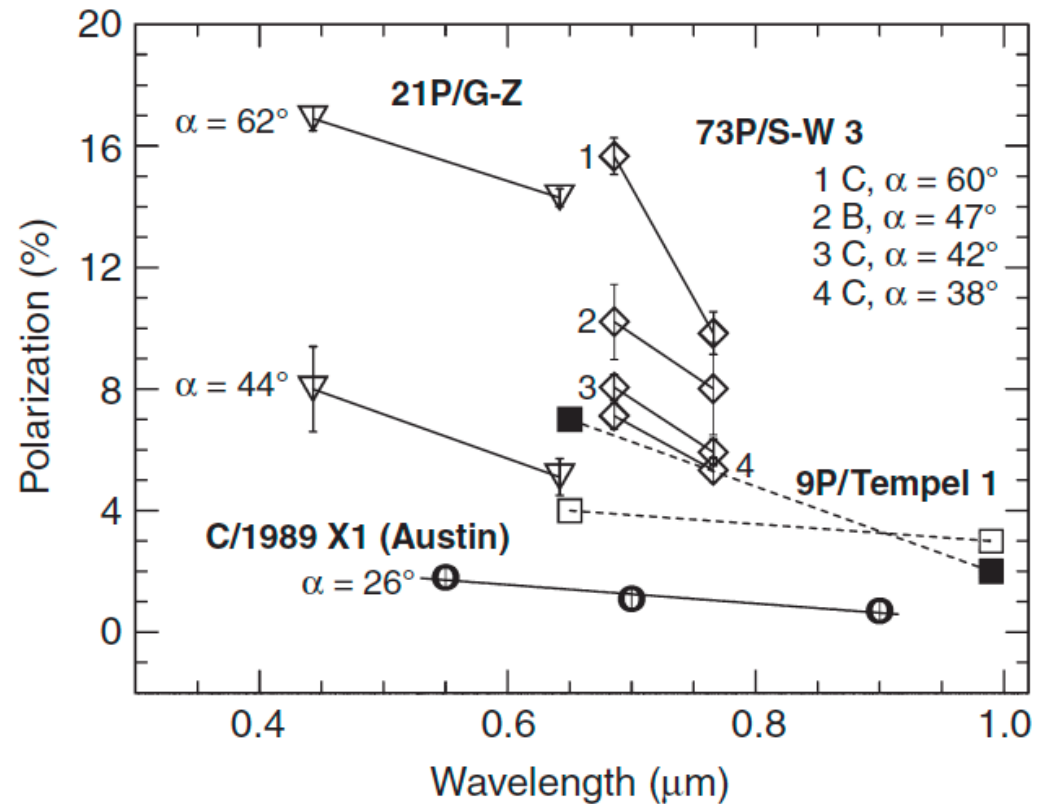


FIGURE 22.5 Non-typical spectral dependences of polarization for comets C/1989 X1 (Austin), 21P/Giacobini–Zinner, B and C fragments of 73P/Schwassmann–Wachmann 3, and 9P/Tempel I at a variety of phase angles. Open and filled squares show polarimetric color of comet 9P/Tempel I, 40 minutes and 1.5 hours after the Deep Impact event, respectively.

TABLE 22.1 Comets with non-typical polarization color

Comet	$\Delta P/\Delta\lambda$ %/μm	Organic comp./ dyn. class, family
GZ	-15	atypical /SP, KB
73P/SW 3	-28	atypical /SP, KB
Tempel 1	$-9 \pm 2 \div -23 \pm 3$	atypical /SP, KB
Austin 89	-7	atypical/DN, OC
S4	-14	atypical/DN, OC

In situ measurements

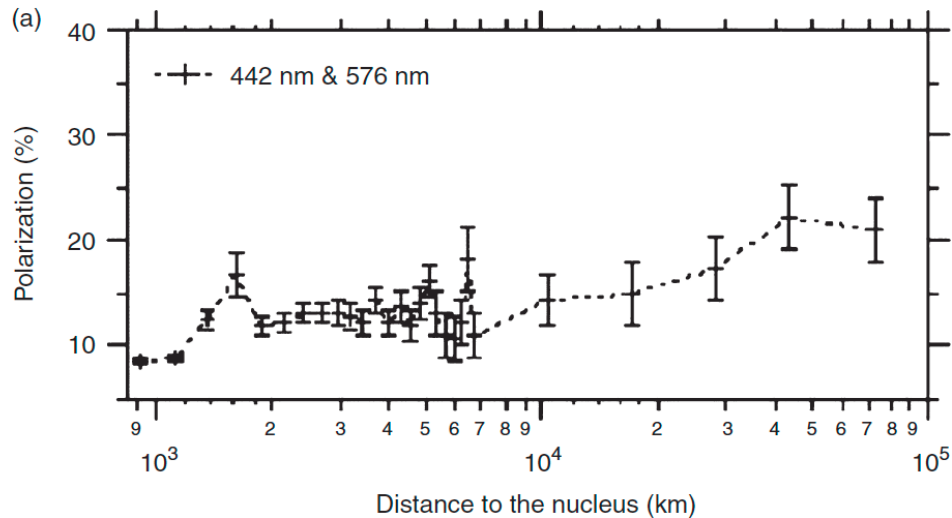
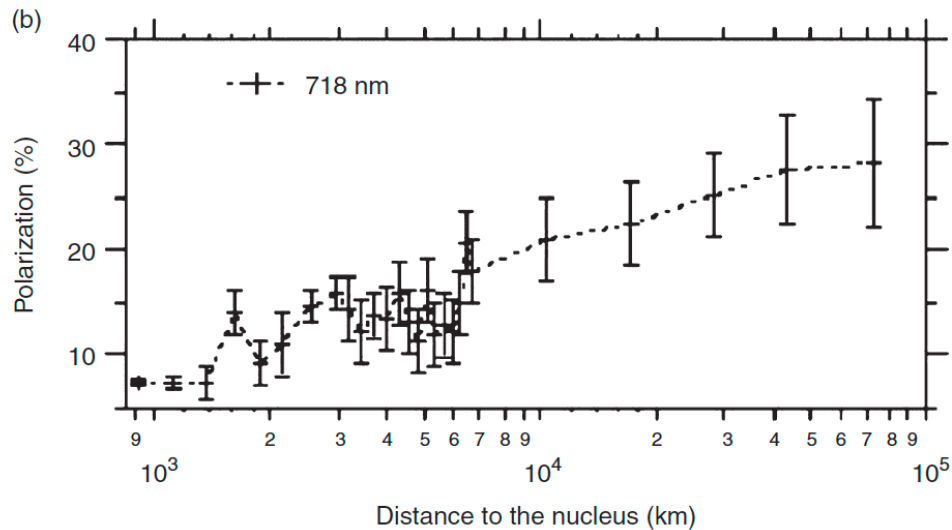


FIGURE 22.6 Changes in linear polarization with distance to the nucleus of 1P/Halley, along the Giotto spacecraft trajectory in the coma. Enhancements are seen at the crossing of jets; polarization is lower in the innermost coma.

From Levasseur-Regourd 2011; reproduced with kind permission from Springer Science and Business Media.



- 1P/Halley monitored with Halley Optical Probe Experiment (HOPE)
- sequential observations along the spacecraft track allow for localized polarization measurement

Distribution of polarization over the coma

- Three different regions were identified for Hale-Bopp
 - background coma
 - polarimetric halo near photocenter (lower positive polarization)
 - jet-like or arc-like features with higher polarization

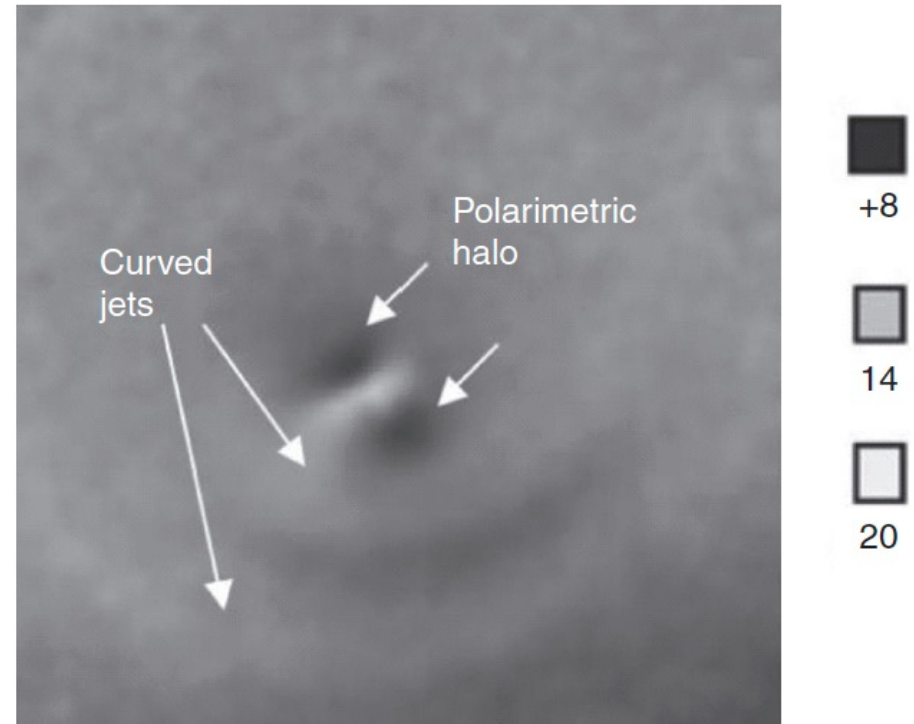


FIGURE 22.7 Polarimetric image of C/1995 O1 (Hale-Bopp) observed in 1997 (field of view 82 000 km²; phase angle 43.6°; red continuum). Variations in dust properties result in a lower polarization halo in the innermost coma and in a higher polarization in the curved jets.

From Levasseur-Regourd (2014).

Specific phenomena in linear polarization

- Outburst and fragmentation events
 - fresh internal material coming to sight
 - variations in polarization observed and modeled
- Stellar occultations
 - nonzero linear polarization detected for zero-polarization stars when observed through comae
 - partially aligned nonspherical dust particles

Interpretation of linear polarization data

- Phase-angle dependence
 - compact regular particles
 - some early success with Mie spheres
 - agglomerates of small grains
 - substantial recent success with DDA and STMM
 - cosmogonic controversies: what can be assumed for the constituents?
 - mixture of compact and aggregated particles
- Spectral dependence
 - Rayleigh scattering, efficiency changes with x^4
 - spectral dependences otherwise hard to conceptualize
- Requirements
 - acceptable photometric and polarimetric fits
 - realistic geometric albedo, color, polarimetric color, and cosmogonic organics/silicates ratio, monomer sizes in aggregates
 - agreement with space mission data for aggregated vs. compact particles

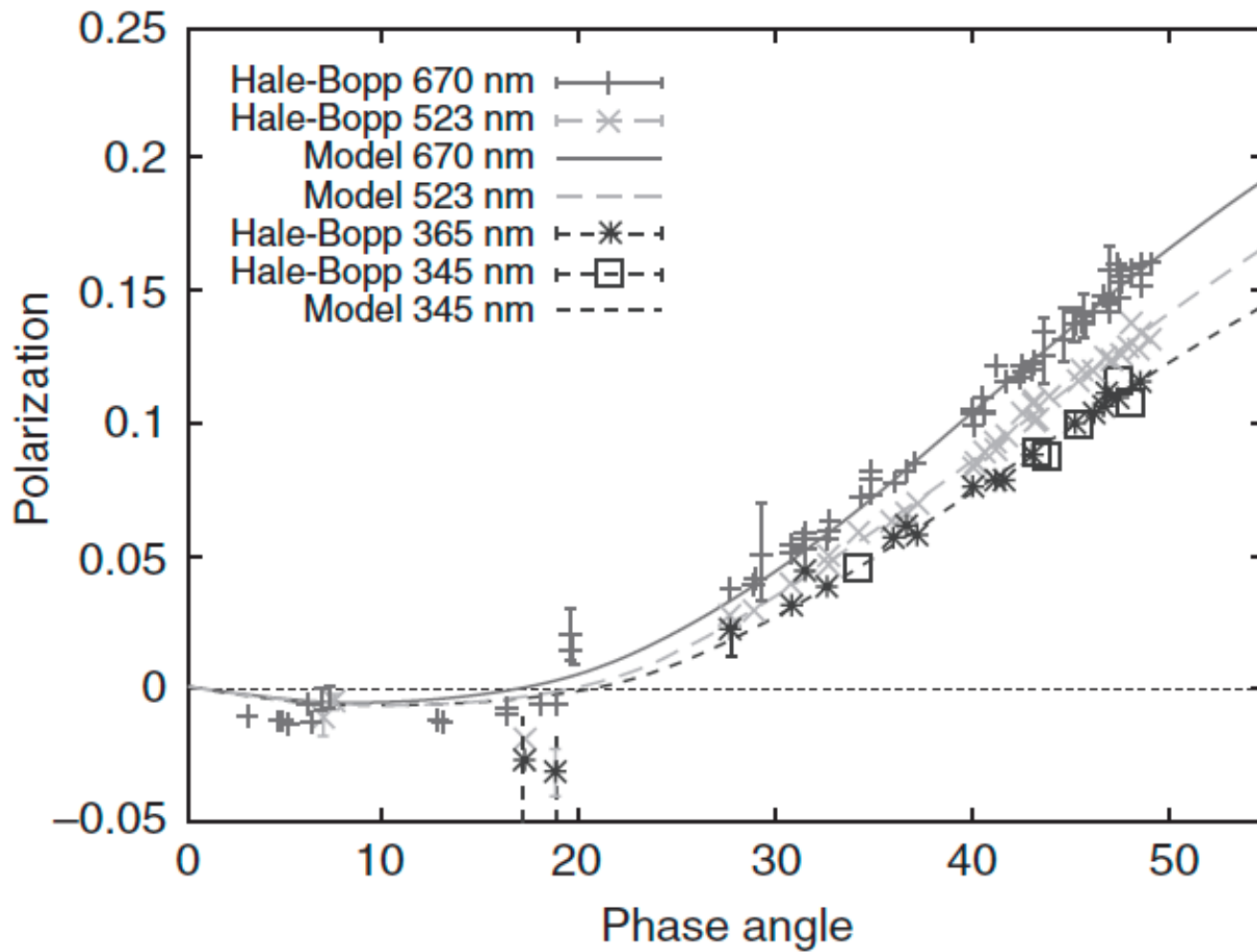


FIGURE 22.8 Observed (symbols) and modeled (lines) dependence of polarization for comet Hale–Bopp for several wavelengths.

From Levasseur-Regourd *et al.* (2008).

Comet nuclei

- Extremely important to study polarimetrically
- 2P/Encke
 - inversion angle agrees with that of F-type asteroids
 - slope at inversion angle substantially higher for F-types
 - red nucleus vs. bluish F-type asteroids
 - nucleus different from any other Solar System object
- 133P/Elst-Pizarro
 - phase-angle dependence similar to F-types

Circular polarization

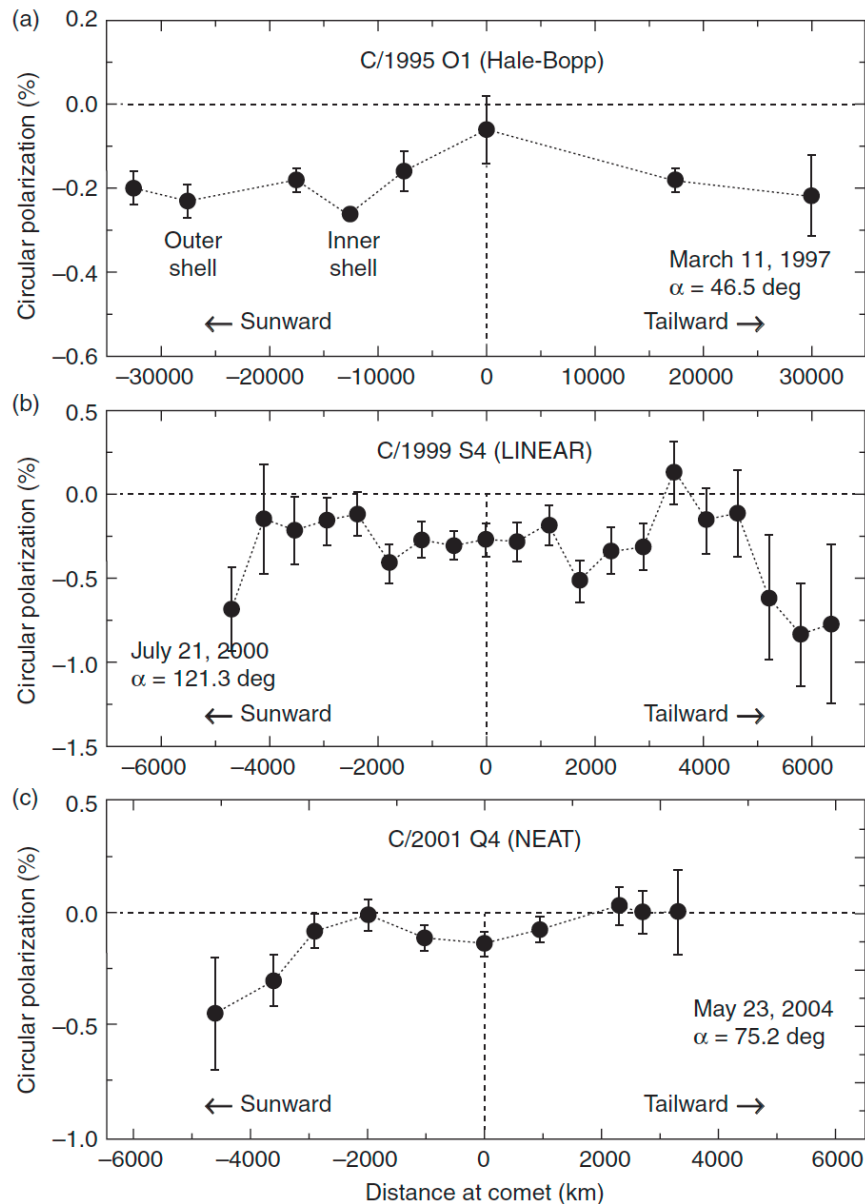


FIGURE 22.9 Variations of the degree of CP along a cut through the coma and nucleus of comets (a) C/1995 O1 (Hale-Bopp); (b) C/1999 S4 (LINEAR); and (c) C/2001 Q4 (NEAT). Error bars indicate the standard deviation of the mean value of polarization.

Reproduced from Mishchenko *et al.* (2010) with kind permission of *Akademiya* of the NAS of Ukraine.

- Confirmed for comets with high confidence
- Difficult to interpret
 - violation of mirror symmetry in the medium or in the scatterers
 - optical activity, presence of chiral molecules
 - no mechanism identified in protoplanetary disks to favor certain handedness

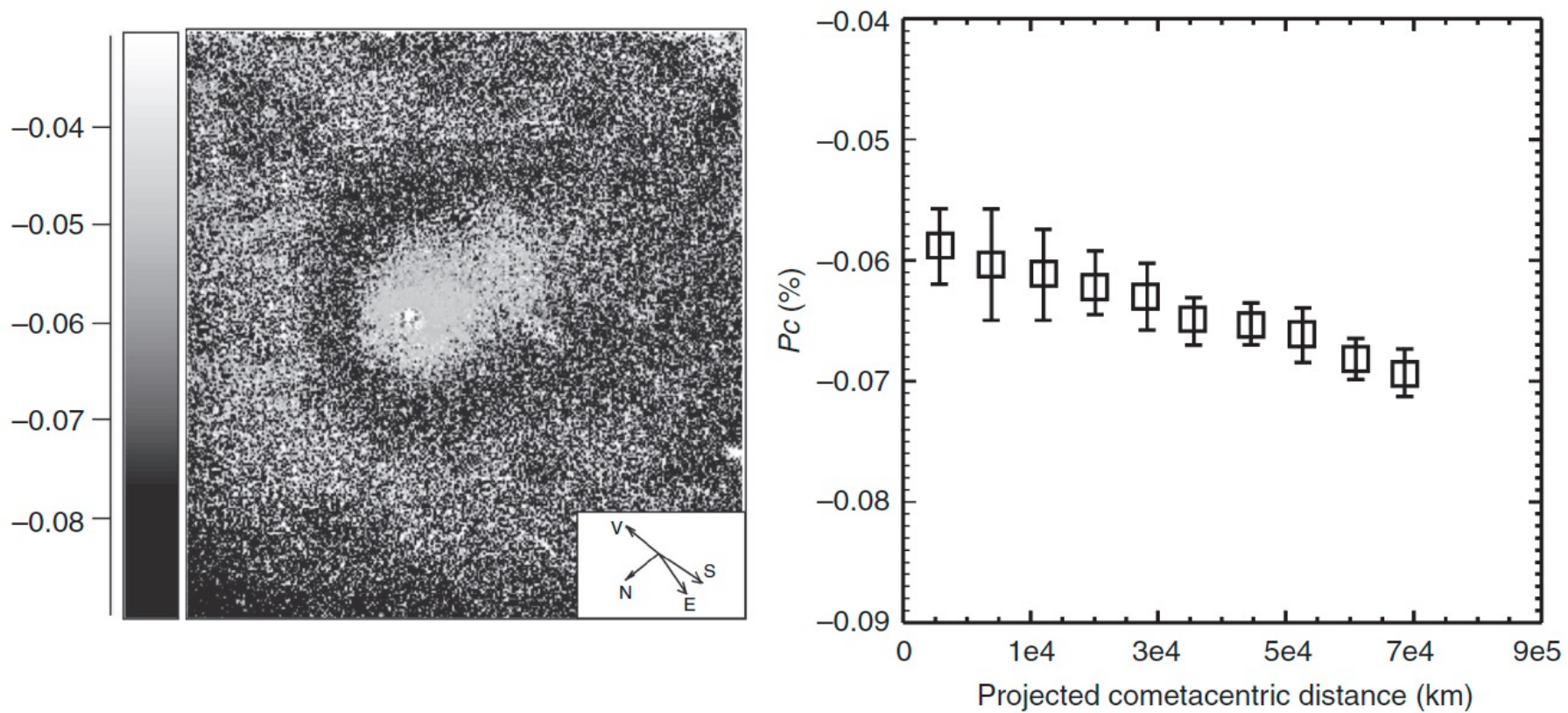


FIGURE 22.10 Circular polarization of comet C/2011 RI (McNaught). Polarization map (left) and an average CP in 20-pixel-wide ($\sim 7''$ at the comet) circular apertures (right) are shown vs. the distance from the comet nucleus.

TABLE 22.2 Mean values of CP in comets

Comet	Year	$P_c \pm \sigma P_c$, %	Phase angle, degrees
Halley ⁶	1986	$(+0.3 \div -0.5) \pm 0.15$	22–41
Hale–Bopp ⁶	1997	$(+0.2 \div -0.26) \pm 0.02$	40–47
S4 LINEAR ⁶	2000	$(+0.7 \div -0.8) \pm 0.07$	61–122
Q4 NEAT	2005	-0.1 ± 0.05	75–77
73P/S–W 3 (B)	2006	-0.2 ± 0.2	92
8P/Tuttle	2008	-0.60 ± 0.07	67.6
9P/Tempel 1	2005	-0.05 ± 0.02	41.2
Garradd	2012	$(-0.07 \div -0.25) \pm 0.02$	35
29P/S–W 1	2012	-0.04 ± 0.01	6.2
PANSTARRS	2013	-0.08 ± 0.01	36
McNaught	2013	-0.07 ± 0.03	12.4

Note: The symbol \div signifies the range between two numbers.

Similarity and diversity of comets: classification issues

- High-polarization vs. low-polarization comets
 - warning: not agreed upon by all researchers
 - dust-to-gas ratio
 - evolution of dust and gas

Conclusions

- Dust aggregate model capable of describing photopolarimetric properties in the bulk comae
- Based on Stardust mission and numerical and experimental simulations, comet dust is likely to consist of dark aggregates and silicate solid particles
- Difference in polarization maxima attributed to the domination of smaller or more porous particles for high-polarization comets and the domination of large compact particles in low-polarization comets
- Nonzero circular polarization discovered in a number of comets but the physical mechanism is under discussion

Perspectives

- **Observations**

- high-resolution spectropolarimetric observations over large phase-angle ranges
- high-resolution polarization and color maps
- time-dependent observations to study evolution

- **Instrumentation**

- polarimeters designed for comets
- polarimeters for space missions (Comet Interceptor has a polarimeter)

- **Interpretation**

- interpretation based on spectral dependences
- consistency with photometric, thermal infrared, dynamic, cosmogonic, in situ data